Published in final edited form as:
Anal Chem. 2005 October 15; 77(20): 6719–6728. doi:10.1021/ac050987t.

Fluoride Selective Optical Sensor Based on Aluminum(III)-Octaethylporphyrin in Thin Polymeric Film: Further Characterization and Practical Application

Ibrahim H. A. Badr[1] and **Mark E. Meyerhoff**[*]
Department of Chemistry, The University of Michigan, 930 N. University, Ann Arbor, MI 48109-1055

Abstract

More detailed analytical studies of a new fluoride selective optical sensor based on the use of aluminum(III)-octaethylporphyrin and a lipophilic pH indicator (4′,5′-dibromofluorescein octadecyl ester; ETH-7075) within a thin plasticized poly(vinyl chloride) film are reported. The sensor exhibits extraordinary optical selectivity for fluoride over a wide range of other anions, including anions with far more positive free energies of hydration (e.g., perchlorate, thiocyanate, nitrate, etc.). UV-VIS spectrophotometric studies of the sensing films indicate that fluoride interacts with the Al(III) center of the porphyrin structure, yielding both a change in the Soret band λ_{max} of the porphyrin as well as a change in the protonation state of the pH indicator within the film. The same change in spectral properties of the metalloporphyrin occurs in the absence of added pH indicator or with added tetraphenylborate derivative anionic sites, but optical responses to fluoride in these cases are shown to be irreversible. The presence of the pH indicator and the simultaneous fluoride/proton coextraction equilibrium chemistry is shown to greatly enhance the reversibility of fluoride binding to the Al(III) porphyrin. Optical response toward fluoride can be observed in the range of 0.1 μM to 1.6 mM. Optical selectivity coefficients of $< 10^{-6}$ for common anions (e.g., sulfate, chloride, nitrate etc.) and $< 10^{-4}$ for perchlorate and thiocyanate are obtained. Measurements of fluoride in drinking water *via* the new optical sensor are shown to correlate well with values obtained for the same samples using a classical LaF_3 based fluoride ion-selective electrode method.

INTRODUCTION

Ever since the development of optical oxygen sensors based on the quenching of the fluorescence of an organic chromophore by dioxygen,[1] the field of optical sensors has evolved in many directions. These include the mode of signal transduction (e.g., absorbance, fluorescence, chemiluminescence, etc.), the nature of the optical device (e.g., fiber optic probes, waveguides, microspheres, etc.), the type of analytes detected (gases, ions, polyions, neutral organics, etc.) and the nature of chemical species used to achieve selective sensing (e.g., indicators, ionophores, enzymes, etc.).[2–8] Compared to electrochemical sensors, optical transduction offers several potential advantages such as continuous real-time remote monitoring capability (using ratiometric methods and/or luminescence lifetime measurements), no need for internal and external reference electrodes or lengthy preconditioning times, and a sensing system that is generally free from electrical noise problems.

*To whom correspondence should be addressed at E-mail: mmeyerho@umich.edu; phone: (734) 763-5916; fax: (734) 647-4865.
[1]On leave from the Department of Chemistry, Faculty of Science, Ain-Shams University, Cairo, Egypt.

Optical sensing polymeric films or so called "bulk-optodes" have been successfully developed for sensitive detection of neutral molecules, gaseous analytes, cations/anions, as well as polyions.[9–12] In the case of optical sensors for ions, many of the same ionophore chemistries used so successfully to prepare polymer membrane type ion-selective electrodes (ISEs) have been employed.[9, 10] Typically, a lipophilic ionophore and a pH chromoionophore are doped within a thin polymeric film. Ionophore selective extraction of the target ion from the sample causes a concomitant coextraction or liberation of protons from/by the pH indicator to maintain charge neutrality within the organic film, yielding a change in the optical properties (e.g., absorption spectrum) of the films.[13]

The development of fluoride selective optical sensors is of potential practical importance and would offer an attractive low-cost/disposable alternative to the widely used solid-state LaF_3 ion-selective electrode, especially for mass production (e.g., via screen printing) of planar sensor arrays and single-use devices. Highly selective fluoride sensors are useful for the determination of fluoride levels in municipal/potable water and for monitoring organofluorophosphates, especially those belonging to a class of highly toxic neurotoxins that are commonly used as chemical warfare agents (e.g., Sarin and Soman). Enzymatic[14] and metal ion[15] catalyzed degradations of these species liberate fluoride ion, which could be detected quickly using a suitable fluoride ion-selective sensor. To date, very few optical sensors have been developed for fluoride ions. Surface optical sensors developed for fluoride ion, based on fluorescence or absorbance/reflectance measurements, suffer from low selectivity and a high detection limit.[16, 17] For example, fluoride optical sensors based on physical immobilization of dyes (e.g., zirconium–calcein blue and alizarine) at the distal end of bifurcated optical fiber showed a high fluoride detection limit (e.g., 2.6×10^{-5} M), long response times, and poor fluoride selectivity over common anions such as sulfate, phosphate and acetate.[16, 17]

The development of highly selective bulk-optode polymeric films for hydrophilic anions, especially fluoride, remains a fundamental challenge. Fluoride has one of the most negative Gibbs free energies of hydration among common anions;[18] thus partitioning of fluoride into an organic polymer phase is thermodynamically unfavorable. Therefore, to devise a bulk-optode for fluoride, a highly selective ion carrier in the organic phase is needed to counterbalance the hydrophilicity of this anion.[19] Recently it was found that polymer membranes doped with Ga(III) and Zr(IV) porphyrins exhibit an enhanced potentiometric selectivity for fluoride due to the ability of these species to interact selectively with fluoride ion *via* a preferred axial ligation reaction.[20–24] Further, it appears that the Ga(III) and Zr(IV) porphyrins may be useful for preparing bulk-optode sensing films for fluoride without the need for addition of a suitable pH indicator, owing to the ability of fluoride ion binding to the respective metal ion centers to alter the equilibrium between monomeric porphyrins and hydroxide ion bridged dimeric porphyrins within the polymeric film.[20–23] The dimer and monomeric species have different Soret band λ_{max} for absorption. However, it has already been observed that Ga(III) and Zr(IV) porphyrin based sensors, in both potentiometric and optical sensing modes, exhibit significant responses toward interferent lipophilic anions such as thiocyanate, salicylate, and iodide,[20–24] making them only marginally useful for analytical purposes, depending on the given application. Very recently, it has been found that thin polymeric films doped with aluminum(III)-octaethylporphyrin and a lipophilic pH-indicator (ETH-7075) yield a significantly enhanced optical fluoride ion selectivity over highly lipophilic anions such as perchlorate, thiocyanate, nitrate, and iodide.[25] Herein, additional detailed studies of this new sensing system are reported to gain more insight into the nature of the fluoride interaction with the aluminum(III)-octaethylporphyrin ionophore. Furthermore, optical fluoride response and selectivity are optimized by examining the effects of membrane plasticizer, amount of chromophores, and pH of the sample solution. Optimized sensing films

are applied for the analysis of fluoride in drinking water, and shown to provide analytical results comparable to measurements made using a solid-state LaF_3 based ISE.

EXPERIMENTAL SECTION

Reagents

4′,5′-Dibromofluorescein octadecyl ester (ETH-7075), high molecular weight poly(vinyl chloride) (PVC), *o*-nitrophenyloctyl ether (*o*-NPOE), dioctylsebacate (DOS), potassium tetrakis[bis-(3,5-trifluoromethyl)phenyl] borate (TFPB) were obtained from Fluka (St. Louis, MO). Chloro-aluminum(III)octaethylporphyrin (Al([OEP]) was obtained from Frontier Scientific (Logan, UT). Sodium salts of fluoride and sulfate were obtained from Mallinckrodt (Phillipsburg, NJ). Glycine, sodium chloride, and sodium bromide were obtained from Fisher Scientific (Cincinnati, OH). Sodium perchlorate, sodium iodide, 2-morpholinoethanesulfonic acid (MES), β-alanine, 1,2-cyclohexanediaminetetraacetic acid (CDTA), and sodium nitrate were purchased from Sigma-Aldrich (St. Louis, MO). Sodium thiocyanate was obtained from J. T. Baker (Philipsburg, NJ). All aqueous solutions were prepared using 18 $M\Omega cm^{-1}$ deionized water produced by a Milli-Q water purification system (Millipore, Bedford, MA).

Preparation of Optically Sensitive Films and Measurement Set-up

The compositions of the various optical films examined in this study are given in Table 1. The optically sensitive films were prepared using a spin-coating technique. Film cocktails were prepared by dissolving the given components in 2 mL of freshly distilled tetrahydrofuran (THF). A dust-free square-shaped quartz plate of about 35 mm in length (Fisher Scientific; Pittsburgh, PA) was positioned by applying a vacuum in a spin coating device (model SCS-G3-8 obtained from Cookson Electronics; Providence, RI). The quartz plate was rotated at 600 rpm, and 100 μL of the polymer film cocktail was injected onto the rotating glass plate. After spinning for ~ 5 s, the quartz plate coated with the optical ion sensing film was removed from the spin coater and dried in air for ~10 min. When not in use, the films were stored in the dark. The thickness of the optical films employed was estimated to be in the range of 1–5 μm depending on the composition of the casting cocktail that was spin coated on the glass plate.[13]

For analytical measurements, the quartz plate coated with the sensing film was mounted in a custom-built spectrophotometer flow-cell similar to that described elsewhere.[26] This cell has an estimated volume of 25 μL when using a Teflon gasket with a 0.14 mm thickness. The flow-cell was mounted into a Perkin-Elmer double beam UV/VIS spectrophotometer (model Lambda 35; Boston, MA). Using a Gilson Minipuls-3 peristaltic pump (Middleton, WI), a buffer was allowed to flow for 20 min at a flow rate of 1.4 mL/min to condition the films. The response of the optical sensing film toward different anions was evaluated by adding known aliquots of the test solution to a stirred reservoir containing 50 mL of buffer. The resulting buffered salt solution was pumped through the cell and re-circulated into the buffer reservoir. After reaching equilibrium, the spectrum of the films was recorded in the range between 350 (or 360) to 630 nm. To correct for the background absorbance, the absorbance measured at 630 nm was subtracted from the absorbance values at the wavelengths of interest. Total fluoride ion concentration (F_T) was used instead of fluoride activity except when experimental data were fitted to theoretical response functions. In the latter case, fluoride ion activity was used. Activity of fluoride in the test buffers was calculated as described elsewhere.[26] ^1H NMR spectra were obtained on a Varian 300 MHz spectrometer in deuterated chloroform.

Analysis of Fluoride in Drinking Water Using Al[OEP] Based Fluoride Optical Film

Ann Arbor, MI, tap-water samples were diluted using β-alanine-phosphate buffer and distilled water to yield samples with different total concentrations of fluoride and a final buffer

composition of 100 mM β-alanine, pH 3.60, and 1 mM in CDTA. The percentage of tap water in the measured samples after dilution was in the range of 20–90 %. Fluoride concentrations in the samples were determined using the Al[OEP] fluoride selective optical sensors after appropriate calibration of the optical sensing films. For comparison purposes, the fluoride levels in the same buffered samples were determined using a classical solid-state LaF_3 ion-selective electrode purchased from Fisher Scientific (Cincinnati, OH).

RESULTS AND DISCUSSION

Previously, it has been shown that the UV-VIS spectral properties of plasticized-polymeric films doped with metalloporphyrins and an appropriate amount of lipophilic charged sites are highly dependent on the concentration of anions that exhibit strong axial ligation with the metal ion center of the metalloporphyrin species used as the ionophore. [21, 22, 27, 28] For example, the UV-VIS absorbance of plasticized polymer films doped with Ga(III) and In(IV) porphyrins is dependent on the concentrations of fluoride and chloride, respectively.[21, 27] Unlike the conventional bulk-optode membranes that require addition of a lipophilic pH-chromoionophore as a signal transducer, the metalloporphyrins in these cases function as both the recognition element as well as a signal transducer *via* the significant spectral changes that occur in the wavelength range of the Soret band. Such spectral changes have been shown to be due to altering a dimer-monomer equilibrium of the metalloporphyrin in the polymer phase by extraction and axial ligation of the preferred anion species.[29, 30]

A comparison of the complex stability constants of fluoride with a variety of metal ions indicates that aluminum(III) forms very stable complexes with fluoride ion in aqueous solution. [31, 32] It is well-documented in the literature that the selectivity of carrier-based optical/electrochemical sensors is highly dependent on the relative binding constants of the primary and interferent ions with the ionophore.[19] This strong affinity of aluminum(III) towards fluoride ion suggests the possibility of using appropriate hydrophobic aluminum(III) complexes as active polymer film components to design useful carrier-based fluoride selective optical and electrochemical sensors.

Spectral Properties of Films Doped with Al[OEP]

In preliminary investigations, the possibility of using Al[OEP] as a fluoride ion selective ionophore in bulk optode type sensors *via* altering the dimer-monomer equilibrium within the organic polymeric phase was examined. The UV-VIS spectra of Al[OEP] based optical films with zero or 50 mol % TFPB (Films 1 and 2; see Table 1 for compositions), measured in 50 mM glycine-phosphate buffer, pH 3.00, exhibit a broadening and significant decrease in the intensity of the Soret band (in range of 375 – 425 nm) in the presence/absence of fluoride ion (see Figure 1). Such behavior has not been observed for any of the previously studied metalloporphyrin-based optical sensing films.[21, 22, 27, 29]. Further, films formulated with Al [OEP] and 25 or 75 mol % TFPB (relative to Al[OEP]) showed similar Soret band attenuation (data not shown). Such a decrease in Soret band intensity and broadening has been observed previously for aluminum(III)-tetraphenylporphyrin encapsulated in a sol-gel matrix and was attributed to the formation of aggregated porphyrin species.[33] In addition, optical spectra of a concentrated solution of aluminum(III)-tetraphenylporphyrin, measured in organic solvent (e.g., ethanol), exhibit a similar Soret band broadening, which was explained by porphyrin aggregation.[33] Indeed, Soret band broadening and molar absorptivity decreases have been reported for variety of porphyrin systems that form aggregates.[34–36] Al[OEP] is more amenable for aggregation compared to aluminum(III)-tetraphenylporphyrin, because the latter is more sterically hindered by the phenyl rings perpendicular to the porphine plane. The optical spectra of the Al[OEP] doped films formulated with 25, 50, or 75 mol % TFPB show a slight

decrease in the absorbance at 404 nm when exposed to 10 mM fluoride ion in 50 mM glycine-phosphate buffer, pH 3.00 (see in Figure 1 for Film-2).

Optical films prepared using 100 mol % TFPB (relative to the Al[OEP]; Film-3), however, exhibit a very sharp and intense Soret band at 404 nm that is typical for most metalloporphyrins. This absorption band at 404 nm can be assigned to the positively charged Al[OEP] monomer. Guilard *et al.* found that the optical spectra of Al[OEP]Cl measured in benzene exhibit a Soret band centered at 399 nm, that is close to that observed with Film-3.[37] Interestingly, it was found that exposing Film-3 to increasing fluoride concentrations prepared in 50 mM glycine-phosphate buffer, pH 3.00, led to a large decrease in the absorption at 404 nm (i.e., monomer band) and a concomitant absorbance increase at 382 nm (see Figure 2). This spectral change is totally different than that observed for other metalloporphyrin systems that exhibit the dimer-monomer equilibrium chemistry, where the dimer consists of a hydroxide ion bridged bis-porphyrin structure. For example, films formulated with Ga(III), In(III) and Zr(IV) porphyrins and appropriate amounts of TFPB (typically near 50 mol %) favor the formation of hydroxide-bridged dimers, that decrease in concentration within the polymer phase as the preferred anionic species is added to the test solution (with a simultaneous increase in the absorbance of the monomer band that is red shifted relative to the dimer).[21, 22, 29] The monohydroxide-bridged dimer of Al[OEP], however, is observed only at relatively high pH-values (pH > 12) (data not shown), indicating that the equilibrium constant for this species is much weaker than the corresponding hydroxide-bridged dimers of Ga(III), In(III), and Zr(IV) porphyrins that are observed in the films even under acidic sample conditions (pH 3).[21, 27]

The new band at 382 nm is likely dimeric porphyrin species in which two fluorides are bridging the Al(III) centers. Fluoride is already known to serve as a bridging ligand with a variety of metal ions, including aluminum ion.[38–41] Since 100 mol % borate is required to observe such behavior (or 100 mol % pH chromoionophore; see below), initial conditioning of the films in buffer leads to all of the TFPB anions serving as counter-ions to 100 % of the Al[OEP] in monomeric form (as $Al[OEP]^+$) and hence the very sharp Soret band expected for the monomer species. As fluoride is added to the buffer, fluoride is extracted to serve as an axial ligand to the $Al[OEP]^+$ species; however, to maintain charge neutrality in the polymeric film, a dimer in which two fluoride ions are bridging two Al[OEP] complexes appears to form $(Al[OEP]F)_2$. If only a single fluoride bridging species were responsible for the dramatic change in UV-VIS spectrum, then 50 mol% TFPB would be the optimal level to stabilize a positively charged $(Al[OEP])_2F^+$ dimer. As fluoride is extracted to form the new dimer, cations from the sample must be coextracted to serve as counter-ions for the lipophilic $TFPB^-$ species.

If the above coextraction chemistry is indeed occurring, then the presence of more lipophilic cations (M^+) in the sample phase should drive the following coextraction reaction to the right, requiring less fluoride ion to decrease the monomer concentration in the polymer film:

$$2\,M^+_{aq} + 2\,F^-_{aq} + 2\,Al[OEP]TFPB_{org} \rightleftarrows (Al[OEP]F)_{2(org)} + 2\,MTFPB_{org} \quad (1)$$

Indeed, when the optical film experiment shown in Figure 2A is carried out using tetrabutylammonium fluoride rather than the sodium salt to increase fluoride level in the sample solution, the change of optical properties (decrease in absorption band at 404 nm) occurs at about three orders of magnitude lower fluoride ion concentration in the sample phase (see data in Figure 1s in the Supporting Information), supporting this concept of coextraction to maintain charge neutrality, and the existence of the dimer of the porphyrin bridged by two fluoride ions.

Kinetics of Optical Response

As shown in the Figure 2 inset, the response time of the Al[OEP] based optical Film-3 towards fluoride ions is very slow with more than 30 min required to reach only 85 % of the equilibrium

optical response when changing fluoride ion concentration from 5 to 48 mM. Furthermore the recovery time of this sensing film is also extremely slow, when changing the sample solution to a fluoride-free buffer after contact with 48 mM fluoride. The observed sluggish response and long recovery times are due to a strong and effectively irreversible binding of fluoride ion to the Al[OEP] ionophore. This strong binding is not surprising based on the high affinity of a hard Lewis acid, aluminum(III), with a hard Lewis base, such as fluoride, and given the known large stability constants for Al(III)-fluoride complexes in aqueous solutions.[31, 32] Furthermore, in a recent study, it was found that an aluminum(III)-salen ionophore within thin polymeric films also exhibits irreversible binding towards fluoride ion in an organic polymeric phase.[26]

It has been reported in the literature that the binding and release kinetics of an ion with an ionophore can be significantly improved by co-incorporation of pH-chromoionophores.[42] For example, a potentiometric lead selective membrane electrode based on lipophilic dithiocarbamate ionophore is poisoned when exposed to aqueous sample solutions containing mercury or silver ions, because of the irreversible binding of such ions to the dithiocarbamate ionophore.[43] Incorporation of a pH-chromoionophore in the membrane phase, in addition to the same dithiocarbamate ionophore, led to fully reversible mercury and silver ion optical sensing systems with a more rapid response time.[43] This improvement in the binding and release kinetics could be attributed to the facilitated release of the analyte metal ion from the polymer phase into the aqueous sample solution phase via an exchange process with hydrogen ion (i.e., hydrogen ion binding with the pH chromoionophore in the organic phase forces the release of the metal ion into the aqueous sample solution to maintain charge neutrality within the film). Hence the overall equilibrium constant for analyte ion extraction is also dictated by the equilibrium constant for the simultaneous protonation of the pH chromoionophore. It is also possible that inter-molecular forces (e.g., hydrogen bonding, π–π interaction, weak ligation etc.) between the added pH-chromoionophore and the ionophore can weaken the ion-ionophore binding, which in turn, leads to faster binding and release kinetics (see UV-VIS and ^{1}H NMR data below).

Therefore, to achieve a better reversibility of the Al[OEP] based fluoride optical sensing film, a lipophilic pH-chromoionophore (ETH-7075) was incorporated in the polymer film at a 100 mol % (relative to the amount of Al[OEP]) (see membrane composition, Film-4, in Table 1). The co-incorporation of the indicator provides new optical transduction wavelengths to monitor fluoride levels. As shown in Figure 3A, addition of fluoride to the sample phase causes protonation of the initially negatively charged ETH-7075 indicator, concomitant with the selective fluoride extraction by the Al[OEP] species, yielding a decrease in the absorbance band corresponding to the deprotonated form of the indicator (λ_{max} = 529 nm) and an increase in absorbance of the band corresponding to the protonated indicator (broad band centered at 475 nm). Further, as shown in Figure 3B, a remarkable improvement in the fluoride response times, as measured in 50 mM glycine-phosphate, pH 3.00, are achieved compared to those obtained using Film-3 (i.e., without the pH-chromoionophore but with 100 mol % of TFPB). Indeed, $t_{90\%}$ (times required to reach 90 % of the equilibrium response) response times of 2 – 7 min for low fluoride concentrations (≤ 22 μM) and less than 1 min for high concentrations (≥0.22 mM) are observed. A $t_{90\%}$ recovery time of 9 min is achieved when changing the sample solution from one containing high fluoride ion concentration (19.8 mM) to a fluoride-free buffer solution (see dashed line in Figure 3B). Measurements using 50 mM MES buffer, pH 5.5, resulted in similar response and recovery times (data not shown). Shorter recovery times, are observed when working in a low fluoride-ion concentration range (i.e., ppm levels), the range that would normally be used for determining fluoride in municipal drinking water samples (see also Figure 3 in ref.[25])

Optical Response of Al[OEP]/ETH-7075 to Fluoride Ion

To achieve greater absorbance changes in response to fluoride ion, the concentrations of the ionophore and the chromoionophore can be increased in the sensing film. Figure 4 shows the changes in the UV-VIS absorption spectrum of Al[OEP]/ETH-7075 based fluoride optical sensing Film-6 (with 72 mmol/Kg of each component) for different fluoride ion concentrations in the wavelength range of 360 – 650 nm. It should be noted that the absorption maximum of Al[OEP] is typically 404 nm in films where only the porphyrin and TFPB are present (see Figure 3, above). However, the Soret band is now observed at 410 nm in the presence of 100 mol % pH-chromoionophore in place of the TFPB. The observed spectral shift of the Al[OEP] in the presence of the pH-chromoionophore suggests some inter-molecular interaction between the two species (e.g., $\pi - \pi$ interaction, etc.). Further studies using ^{1}H NMR spectroscopy support the existence of such an interaction between the pH-chromoionophore (ETH-7075) and Al[OEP]. The meso-protons of the porphyrin ring of Al[OEP] are shifted up-field when ETH-7075 is added to deuterated chloroform solution of Al[OEP] (see Figure 2s in the Supporting Information). It can be also seen in Figure 2s that the ^{1}H NMR spectra of the pH-chromoionophore changes significantly and all peaks are shifted up-field and broadened when the chromoionophore is mixed with Al[OEP].

As can be seen in Figure 4, parallel to the change in the absorbance spectra of the pH-chromoionophore in the wavelength range 450 – 600 nm, significant absorbance changes of the Soret band also occur in the wavelength range 360–425 nm. At low fluoride ion concentrations (≤70 μM) there is a remarkable decrease in the absorbance of the Soret band of the Al[OEP] monomer at 410 nm (see Figure 4 inset for a blow-up of the spectral change at the Soret band). This decrease in the monomer band is accompanied by an increase in the absorbance of a broad band in the wavelength range of 360 – 400 nm that is blue shifted relative to the monomer peak. Similar to Film-3 (i.e., with TFPB added, but without the pH chromoionophore) this absorption band could be assigned to a bis-fluoride bridged dimer as discussed above for the spectral response of sensors based on Film-3. However, since the coextraction of protons is now more favorable due to the presence of ETH-7075 in the polymeric film, the concentrations of fluoride required to obtain significant optical response are now much lower than in the case of using $TFPB^-$ as the initial counter-ion to $Al[OEP]^+$ in the film. At higher fluoride ion concentrations (> 70 μM), however, the absorbance of the monomer band displays a slight increase with a λ_{max} at 407 nm. This overall spectral behavior points to the possible existence of multiple equlibria in which a bis-fluoride bridged porphyrin dimer is initially formed upon increasing fluoride levels in the low concentration range, with other species formed at higher concentrations. Attempts to fit the experimental data obtained to response functions derived based on various modes of equilibria led to poor curve fittings (data not shown). Interestingly, we found that the experimental data obtained for different film compositions and measured at different pH-values or different buffer systems fit very well with the general optode response function assuming a 1 F^-:1 Al[OEP]: 1 [Ind^-] stoichiometry and an equimolar ratio of Al[OEP] to ETH-7075 in the membrane phase (see Figures 5A, B, C, and D, as well as Figure 6B for Film-7 formulated with DOS). The theoretical curves in this case can be calculated based on the following general anion-optode response function[13]:

$$K = \frac{1}{a_{H^+} a_{F^-}} \cdot \frac{(1-\alpha)^2}{\alpha^2} \quad (2)$$

where (K) corresponding to the overall coextraction constant, and α -value (the degree of deprotonation) is the fraction of the total indicator present in the deprotonated form.[13]

Although it appears from the spectral data that the Al[OEP]-fluoride interaction is not as simple as that observed for other porphyrin systems, and possibly involves multiple equlibria including the formation of a bis-fluoride bridged porphyrin dimer, the fluoride ion response of the optical

sensitive films based on Al[OEP] does follow the classical optode response function for a 1:1 complex formation. This would be expected even if the neutral bis-fluoride bridged dimer is the major product after extraction of fluoride ions.[13] Confirmation of the exact structures of the key species involved in Al[OEP]-fluoride interaction by spectroscopic methods (e.g., fluorine/aluminum NMR spectroscopy), and x-ray crystallography is currently underway in this laboratory.

Optical Fluoride Selectivity

Figure 6A and the data in Table 2 illustrate that Al[OEP] based optical sensors exhibit an extraordinarily high selectivity for fluoride ion over the most lipophilic anions such as perchlorate, thiocyanate, and other environmentally relevant anions (e.g., chloride, nitrate, and sulfate). The Al[OEP]/ETH-7075 based fluoride optical sensor yields far better selectivity than previously reported Zr(IV) and Ga(III) porphyrin based potentiometric sensors by 4 orders of magnitude in the cases of perchlorate, thiocyanate, and nitrate (see Table 2). The comparison between optical and potentiometric selectivity is acceptable because both selectivity terms (K_{ij}^{pot}, K_{ij}^{opt}) are based on the Nicolskii-Eisenman definition.[44]

As mentioned previously, a relatively low fluoride ion concentration (≤70 μM) results in a large decrease in the absorbance at the Soret band at 410 nm even when the pH chromoionophore is present in the sensing film (see data in Figure 4). Interestingly, these changes were also found to be highly selective for fluoride with little or no optical responses for most anions and minimal response toward perchlorate (see Figure 3s in the Supporting Information). Calculation of the selectivity coefficients based on the absorbance changes of the Soret band, however, requires a better understanding of the nature of the interaction of the fluoride ion to the Al[OEP]. In contrast, monitoring absorbance changes of the pH indicator that arises from the proton coextraction process provides a more useful and meaningful measure of true anion selectivity coefficients for this system.

The selectivity of Al[OEP]/ETH-7075 based fluoride optical sensing film easily meets the selectivity requirement for analysis of fluoride in municipal drinking water samples with 1 % error limits (see data in Table 2). The required selectivity coefficients for analysis in municipal drinking water indicated in this table were calculated using a method similar to that reported by Oesch *et al.*,[45] taking into consideration the effect of the charge of primary and interfering ions.[46] The required selectivity values for the worst case (i.e., lowest concentration of fluoride and highest concentration of interferent ion), $K_{i.j,worst\ case}^{Opt}$, were determined according to the eq. (3),

$$K_{i,j,worst\ case}^{Opt} = \frac{a_{i,low}}{(a_{j,high})^{z_i/z_j}} \cdot \left(\frac{P_{ij}}{100}\right)^{z_i/z_j} \quad (3)$$

where, $a_{j,\ high}$ is the maximum concomitant level (MCL) of the interfering species as set by the U.S. Environmental Protection Agency (U.S. EPA),[47] $a_{i,\ low}$ is the lowest level of fluoride in municipal drinking water as set by EPA,[47] p_{ij} is the maximal tolerated error (%) caused by the interferent ion j^{zj} (this was set to 1 %), and z_i, z_j are the charges of i and j, respectively.

Effect of Film Plasticizer

The effect of plasticizer type on the selectivity of the fluoride optical sensing films based on Al[OEP]/ETH-7075 was also investigated. As shown in Figure 6B and Table 2, Al[OEP]/ ETH-7075 based fluoride optical films formulated with DOS (Film-7) exhibit inferior fluoride ion selectivity compared to membranes formulated with o-NPOE. For both optical and potentiometric ion sensors, the dependence of the selectivity on the nature of plasticizer is often

reported in the literature.[48] Although there is no general rule or a mathematical model that can predict the effect of given plasticizers on the response characteristics of the sensors, the observed effects are likely due to a change in the relative binding constants of primary and interferent ions with the metalloporphyrin due to the change in the dielectric constant of the polymeric film. The effect of plasticizer is even more pronounced for carrier-based optical/potentiometric sensors based on metalloporphyrins that involve formation of dimer species.[49] Such dimer species have been observed to be more stable when formulating films with high dielectric constant plasticizers.[50] Al[OEP]/ETH-7075 based optical films prepared with *o*-NPOE also exhibit faster response, especially at low fluoride concentrations, when compared to that obtained with optical films formulated with DOS as the plasticizer (see Figures 4s A & B in the Supporting Information). It should be noted that the response and recovery times obtained with Film-6, are longer than that obtained using Film-3. This is because optical films cast using Film-6 cocktail are somewhat thicker due to increased levels of ionophore and chromoionophore agents, and this is expected to yield a longer equilibration time with the sample solution. In general, the response and recovery times obtained using Al[OEP]/ETH-7075 optical films are somewhat slower than normally expected for optode films with the same thickness (i.e., on the order of few seconds).[13] This slow response and recovery could be explained based on the strong interaction of fluoride to the aluminum metal ion center as indicated by the high coextraction constant obtained ($\log K = 7.8 \pm 0.2$). Indeed, fluoride optical response and recovery times obtained with a submicron thick film, Film-3, using a waveguide-setup, modified after *Toth et al*,[51] resulted in response and recovery times similar to that obtained with 1 – 2 μm thick film (data not shown). This observation reveals that the response and recovery times of Al[OEP] based optical sensors are limited by the binding and release kinetics of fluoride with the Al(III) center of the OEP and not by the diffusional processes within the polymeric film in case of very thin films (< 1–2 μm). In general, fluoride sensitive films based on Al[OEP]/ETH-7075 and prepared using o-NPOE exhibit better fluoride selectivity and response/recovery times compared to those prepared using DOS. Therefore, optically sensitive fluoride films based on Al[OEP]/ETH-7075 and prepared using o-NPOE were selected for analysis of fluoride in municipal drinking water.

Measurements of Fluoride in Drinking Water

As described above, the sensitivity of Al[OEP]/ETH-7075 based fluoride optical sensitive film can be enhanced by increasing the amount of chromophores in the polymeric film phase. As shown in Figure 7, compared to optical films formulated using 16 mmol/Kg Al[OEP]/ETH-7075, the sensitivities ($\Delta A/\Delta C$) of films formulated with 24, 72 mmol/Kg of Al[OEP]/ETH-7075 are improved by 3 and 13 fold, respectively. Therefore for fluoride analysis in municipal drinking water was performed using films formulated with a 72 mmol/Kg of active ingredients (Film-6).

The standard method for the analysis of fluoride ion in drinking water using the LaF_3 electrode requires the use of a strong chelating agents such as CDTA at pH 5.5 to eliminate any possible interferences from metal ions (e.g., Al^{3+} and Fe^{3+}).[52, 53] This buffer, however, is not suitable when employing the Al[OEP]/ETH7075 based fluoride optical sensing films due to the strong pH interference originating from the pH cross-reactivity of the pH-chromoionophore based optical sensors. Therefore, several buffer systems were examined for fluoride analysis using the standard ISE method to adapt a buffer system that is efficient in masking of the interferent metal ions and also has a low pH-value. The buffers examined included 100 mM β-alanine-phosphate, 1 mM in CDTA, pH 3.6, (buffer-1); 100 mM glycine-phosphate,1 mM in CDTA, pH 3.6 (buffer-2); 0.05 M glycine-phosphate, pH 3.00 (buffer-3); and 100 mM glycine-phosphate, pH 3.00 (buffer-4). The fluoride recovery obtained in different buffers was compared to that found using the TISAB buffer (i.e., total ionic strength adjustor buffer (acetate buffer) containing CDTA at pH 5.5, which reflects full fluoride recovery[54]). Only buffer-1,

and buffer-2 yielded a complete fluoride ion recovery (i.e., similar to that achieved using the TISAB buffer). Buffer-1 was selected for the analysis of fluoride in municipal drinking water using the Al[OEP]/ETH-7075 based fluoride optical sensing film. Water samples were diluted with buffer and distilled water to yield different fluoride ion concentration levels in a final buffer concentration of 100 mM β-alanine, pH 3.6, 1 mM CDTA. As shown in Table 3, data obtained using the Al[OEP]/ETH-7075 fluoride optical sensor are comparable to those obtained using the standard LaF_3 ion-selective electrode.

CONCLUSIONS

More details regarding the chemistry and analytical response properties of a very promising new fluoride selective optical sensor have been provided herein. The sensor is based on use of an aluminum(III)-octaethylporphyrin and a lipophilic pH indicator within an *o*-NPOE plasticized-PVC film. Although films prepared with the porphyrin and lipophilic anion sites in the form of borate derivatives also exhibit optical fluoride response, the response times and reversibility of such a system are poor. The presence of the pH indicator enhances the kinetics of fluoride response significantly. The optical fluoride ion selectivity of the optimized film composition is substantially greater than any previously reported optical or electrochemical fluoride sensors based on ionophores in polymer membranes/films. While demonstrated here as a suitable transducer for determination of fluoride levels in water samples, it is likely that this new optical fluoride sensor can readily be adapted for a wide range of other applications in which simple detection of fluoride ions within samples is needed, or in coupled reactions that liberate fluoride ion from given organic analytes (e.g., pesticides, nerve gases, etc.). Further, it is likely that the same chemistry used here to create a useful optical fluoride selective sensor can be adapted to the design of a new fluoride selective polymer membrane electrode. Such efforts are currently ongoing in this laboratory.

Supplementary Material

Refer to Web version on PubMed Central for supplementary material.

Acknowledgements

We gratefully acknowledge the National Institute of Health, grant number EB 000784 for support of this work. IHAB thanks Ain-Shams University, Cairo, Egypt for granting a sabbatical leave. The authors thank Mr. Youngjae Kang for his help in performing the waveguide experiment.

References

1. Bergman I. Nature 1968;218:396.
2. Oldham PB, McCarroll ME, McGown LB, Warner IM. Anal Chem 2000;72:197–209.
3. Kuswandi B, Andres R, Narayanaswamy R. Analyst 2001;126:1469–1491. [PubMed: 11534629]
4. Suksai C, Tuntulani T. Chem Soc Rev 2003;32:192–202. [PubMed: 12875025]
5. Johnson RD, Bachas LG. Anal Bioanal Chem 2003;376:328–341. [PubMed: 12734632]
6. Aylott JW. Analyst 2003;128:309–312. [PubMed: 12741632]
7. Wolfbeis OS. Anal Chem 2004;76:3269–3284. [PubMed: 15193108]
8. Biran I, Walt DR. Opt Biosens 2002:5–56.
9. Buehlmann P, Pretsch E, Bakker E. Chem Rev 1998;98:1593–1687. [PubMed: 11848943]
10. Spichiger-Keller, UE. Chemical Sensors and Biosensors for Medical and Biological Applications. Wiley-VCH: Weinheim; 1998.
11. Wang E, Meyerhoff ME, Yang VC. Anal Chem 1995;67:522–527. [PubMed: 7893001]
12. Dai S, Ye Q, Wang E, Meyerhoff ME. Anal Chem 2000;72:3142–3149. [PubMed: 10939379]
13. Seiler K, Simon W. Anal Chim Acta 1992;266:73–81.

14. Landis, WG.; DeFrank, JJ. Biotechnol Biodegrad. 4. 1990. Advances in Applied Biotechnology Series; p. 183-201.
15. Wagner-Jauregg T, Hackley BE Jr, Lies TA, Owens OO, Proper R. J Am Chem Soc 1955;77:922–929.
16. Russell DA, Narayanaswamy R. Analyst 1989;114:381–385.
17. Narayanaswamy R, Russell DA, Sevilla F. Talanta 1988;35:83–88.
18. Zhan CG, Dixon DA. J Phys Chem A 2004;108:2020–2029.
19. Morf, WE. The Principles of Ion-Selective Electrodes and Membrane Transpot. Elsevier: New York; 1981.
20. Steinle ED, Schaller U, Meyerhoff ME. Anal Sci 1998;14:79–84.
21. Malinowska E, Niedziolka J, Meyerhoff ME. Anal Chim Acta 2001;432:67–78.
22. Malinowska E, Gorski L, Meyerhoff ME. Anal Chim Acta 2002;468:133–141.
23. Gorski L, Meyerhoff ME, Malinowska E. Talanta 2004;63:101–107.
24. Gorski L, Malinowska E. Anal Chim Acta 2005;540:159–165.
25. Badr IHA, Meyerhoff ME. J Am Chem Soc 2005;127:5318–5319. [PubMed: 15826159]
26. Badr IHA, Meyerhoff ME. Anal Chim Acta. 2005Submitted
27. Zhang W, Rozniecka E, Malinowska E, Parzuchowski P, Meyerhoff ME. Anal Chem 2002;74:4548–4557. [PubMed: 12236368]
28. Qin W, Parzuchowski P, Zhang W, Meyerhoff ME. Anal Chem 2003;75:332–340. [PubMed: 12553770]
29. Steinle ED, Amemiya S, Buehlmann P, Meyerhoff ME. Anal Chem 2000;72:5766–5773. [PubMed: 11128934]
30. Parzuchowski PG, Kampf JW, Rozniecka E, Kondratenko Y, Malinowska E, Meyerhoff ME. Inorg Chim Acta 2003;355:302–313.
31. Smith, RM.; Martell, AE. Inorganic Complexes. 4. Plenum; New York: 1974. Critical Stability Constants.
32. Kotrly, S.; Sucha, L. Handbook of Chemical Equilibria in Analytical Chemistry. Wiley; New York: 1985.
33. Hungerford G, Pereira MR, Ferreira JA, Viseu TMR, Coelho AF, Isabel M, Ferreira C, Suhling K. J Fluores 2002;12:397–417.
34. Togashi DM, Costa SMB, Sobral AJFN, Gonsalves AMR. J Phys Chem B 2004;108:11344–11356.
35. Fukushima K, Funatsu K, Ichimura A, Sasaki Y, Suzuki M, Fujihara T, Tsuge K, Imamura T. Inorg Chem 2003;42:3187–3193. [PubMed: 12739958]
36. Komatsu T, Yanagimoto T, Furubayashi Y, Wu J, Tsuchida E. Langmuir 1999;15:4427–4433.
37. Guilard R, Zrineh A, Tabard A, Endo A, Han BC, Lecomte C, Souhassou M, Habbou A, Ferhat M, Kadish KM. Inorg Chem 1990;29:4476–4482.
38. Downs, AJ., editor. Chemistry of Aluminum, Gallium, Indium and Thallium. Chapman & Hall; Glasgow: 1993.
39. Becker C, Kieltsch I, Broggini D, Mezzetti A. Inorg Chem 2003;42:8417–8429. [PubMed: 14658895]
40. Arndt P, Spannenberg A, Baumann W, Burlakov VV, Rosenthal U, Becke S, Weiss T. Organometallics 2004;23:4792–4795.
41. Grushin VV, Marshall WJ. J Am Chem Soc 2004;126:3068–3069. [PubMed: 15012134]
42. Lerchi M, Reitter E, Simon W, Pretsch E, Chowdhury DA, Kamata S. Anal Chem 1994;66:1713–1717.
43. Kamata S, Onoyama K. Anal Chem 1991;63:1295–1298.
44. Bakker E, Buehlmann P, Pretsch E. Chem Rev 1997;97:3083–3132. [PubMed: 11851486]
45. Oesch U, Ammann D, Pham HV, Wuthier U, Zuend R, Simon W. J Chem Soc Faraday Trans 1 1986;82:1179–1186.
46. Bakker E, Meruva RK, Pretsch E, Meyerhoff ME. Anal Chem 1994;66:3021–3030. [PubMed: 7978299]

47. U.S. Environmental Protection Agency. Current Drinking Water Standards, EPA 816-F-02-013. Washington, DC: U.S. Environmental Protection Agency, Office of Water; Jul. 2002

48. Eugster R, Rosatzin T, Rusterholz B, Aebersold B, Pedrazza U, Rueegg D, Schmid A, Spichiger UE, Simon W. Anal Chim Acta 1994;289:1–13.

49. Gorski L, Malinowska E, Parzuchowski P, Zhang W, Meyerhoff ME. Electroanal 2003;15:1229–1235.

50. Dolphin, D., editor. The Porphyrins. 5. Academic Press; New York: 1978.

51. Toth K, Nagy G, Thi Thu Lan B, Jeney J, Choquette SJ. Anal Chim Acta 1997;353:1–10.

52. ASTM American Society for Testing and Materials. 1991 Annual Book of ASTM Standards, Section 2: Water and Environmental Technology, Vol. 11.01: Water (II); D1179-D1188. ASTM; West Conshohocken, PA: 1991.

53. ASTM International. Standard Test Methods for Fluoride Ion in Water; D1179-04. ASTM; West Conshohocken, PA: 2005.

54. Harwood JE. Water Research 1969;3:273–280.

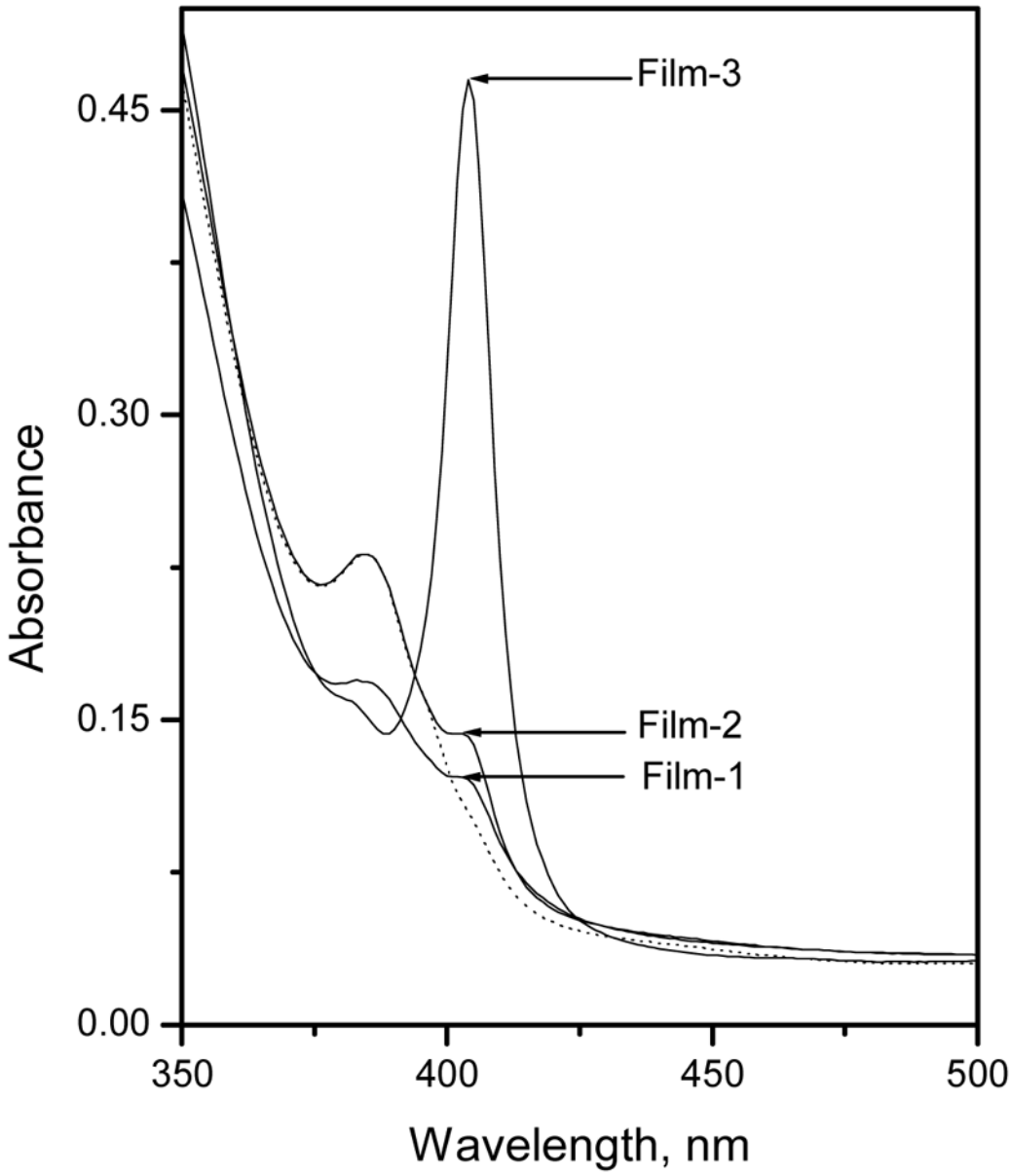

Fig. 1.

Absorption spectra of Al[OEP] based optical Films 1, 2, and 3 measured in 50 mM glycine-phosphate buffer, pH 3.00. Dashed line represents the optical spectra of Film-2 when exposed to 10 mM fluoride ion concentration prepared in the same buffer.

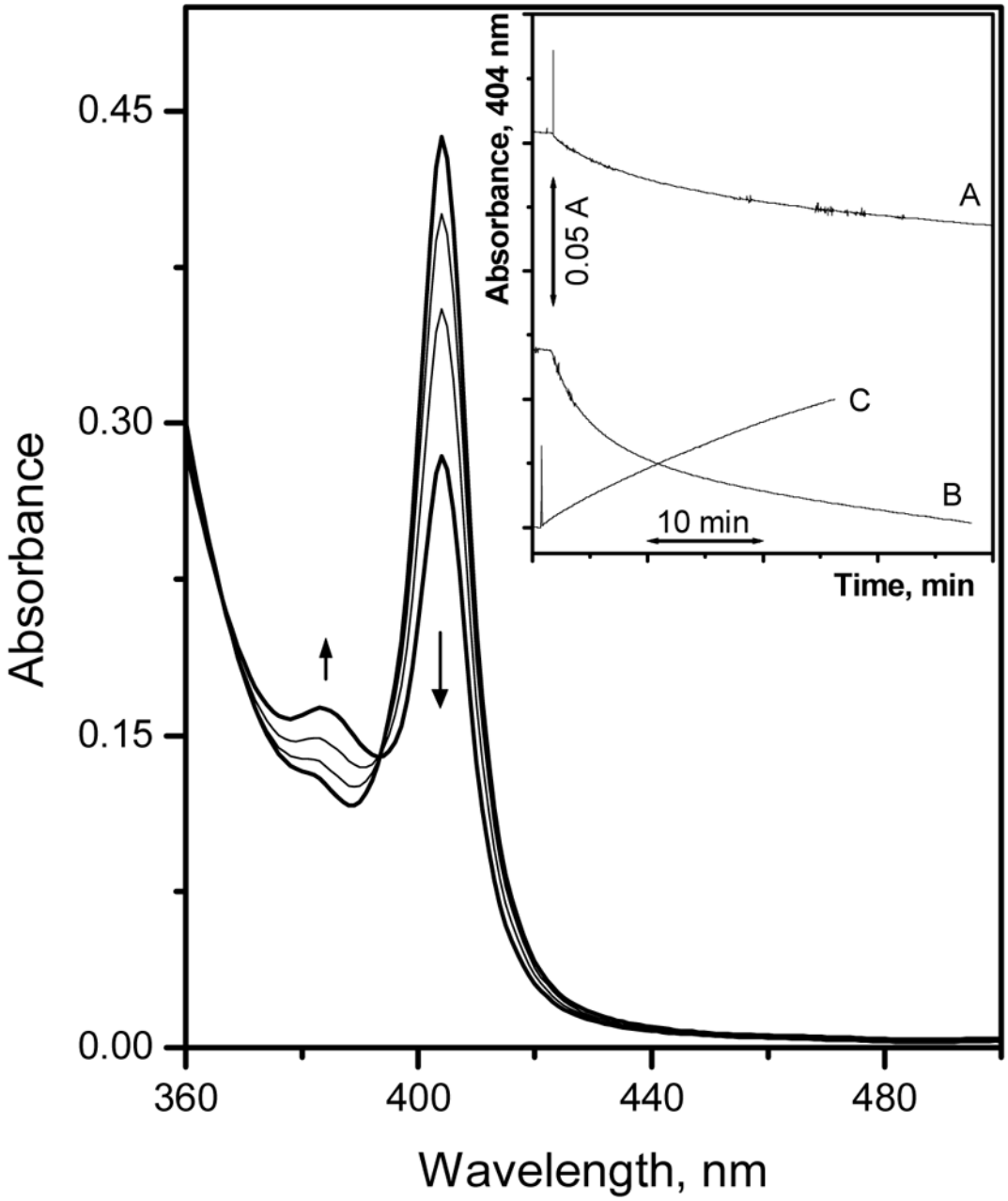

Fig. 2.

Absorption spectra of Film-3, measured in 50 mM glycine-phosphate buffer, pH 3.00, equilibrated with different fluoride concentrations: 5.5 μM, 0.53, 5.0, and 48 mM (from top to bottom at 404 nm). The inset shows the fluoride response time trace when changing the fluoride concentration from 5.5 μM to 0.53 mM (A), 5.0 to 48 mM (B), and the recovery time when changing the sample from 48 mM fluoride to buffer free from fluoride ions(C).

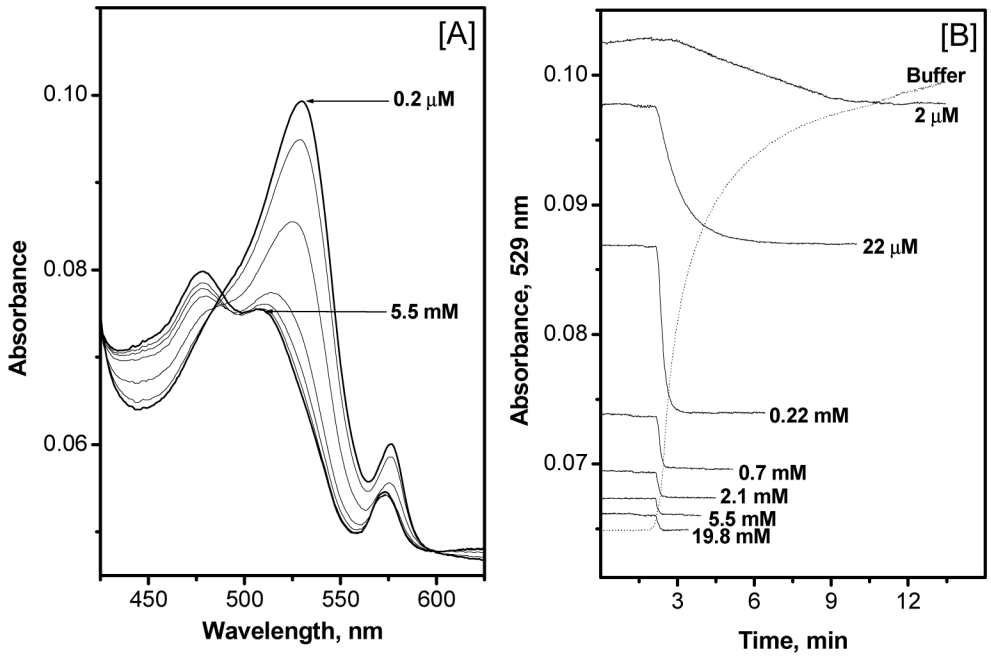

Fig. 3.

[A] Absorption spectra of Film 4 measured in 50 mM glycine-phosphate buffer, pH 3.00, and at varying fluoride ion concentrations: 0.2, 2, and 22 μM, and 0.22, 0.7, 2.1, and 5.5 mM. The peak absorbance at 529 nm decreased monotonically with increasing fluoride concentration. [B] Typical response time of Al[OEP]/ETH-7075 sensing Film-4, measured in 50 mM glycine-phosphate buffer, pH 3.00, at different fluoride concentrations. Dashed line represents the recovery time when changing the sample from 19.8 mM to fluoride-free buffer solution.

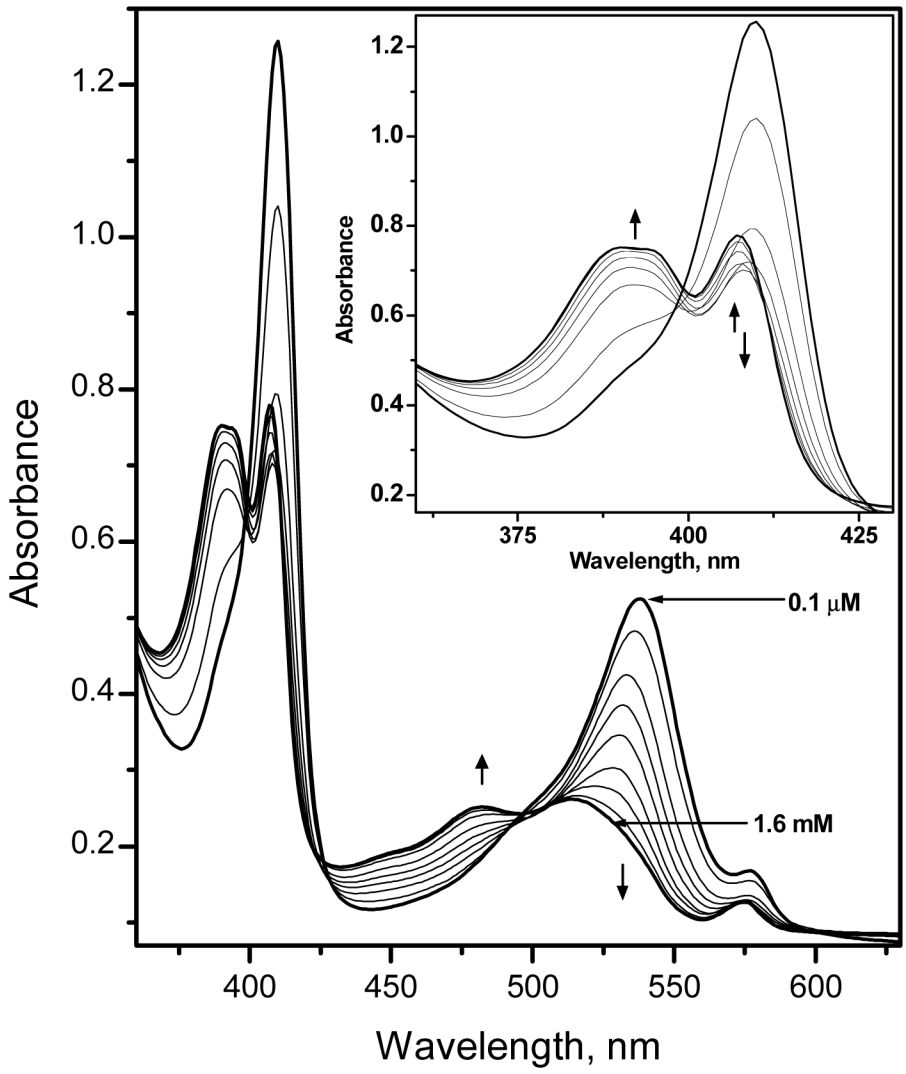

Fig. 4.

Absorption spectra of Film-6 measured in 50 mM glycine-phosphate buffer, pH 3.00, and at varying fluoride concentrations: 0.1, 1.0, 11, 31, and 71 μM, and 0.17, 0.36, 10.8 and 1.6 mM. The inset is a blow-up of the spectral changes that occur in the Soret band region of the spectrum.

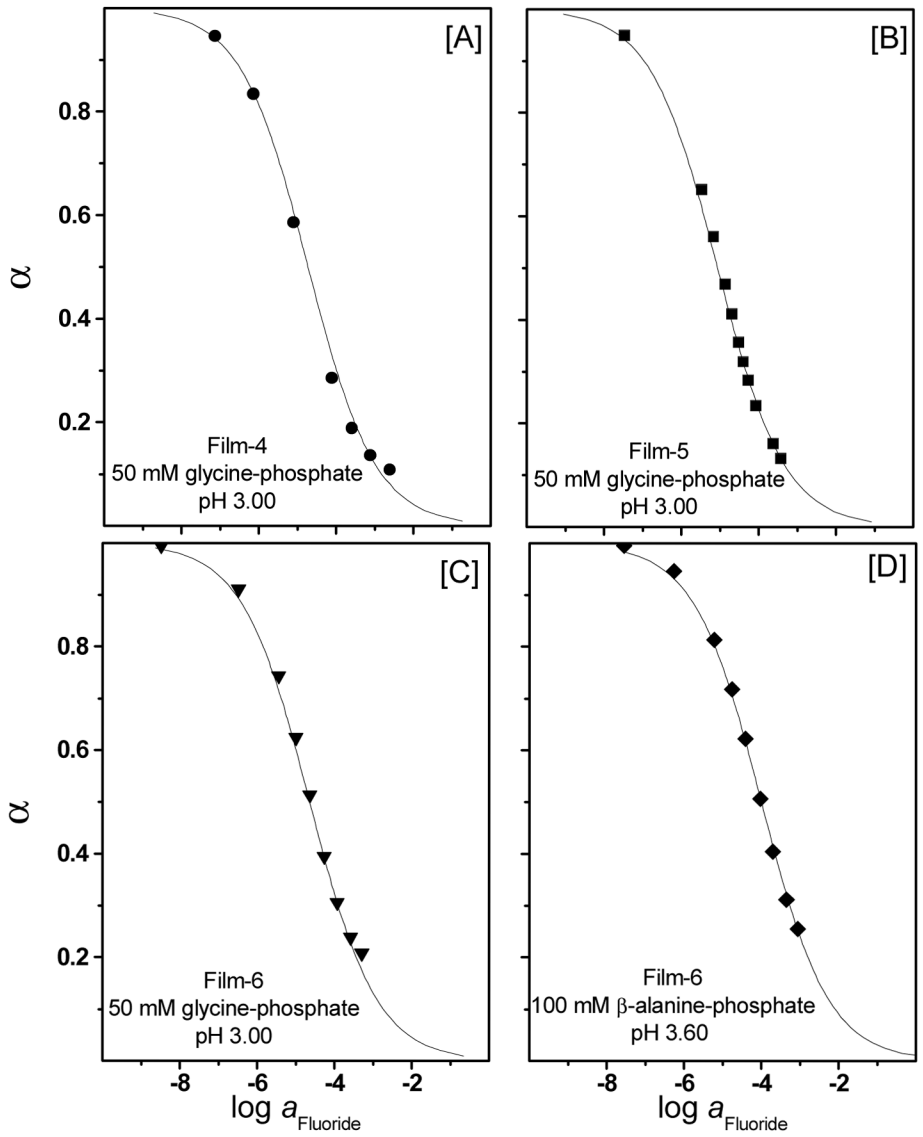

Fig. 5.

Optical response of the Al[OEP]/ETH-7075 based fluoride optical sensitive films as a function of fluoride ion concentrations at different pH values and different membrane compositions. The solid lines are the theoretical response curves based on eq. 2.

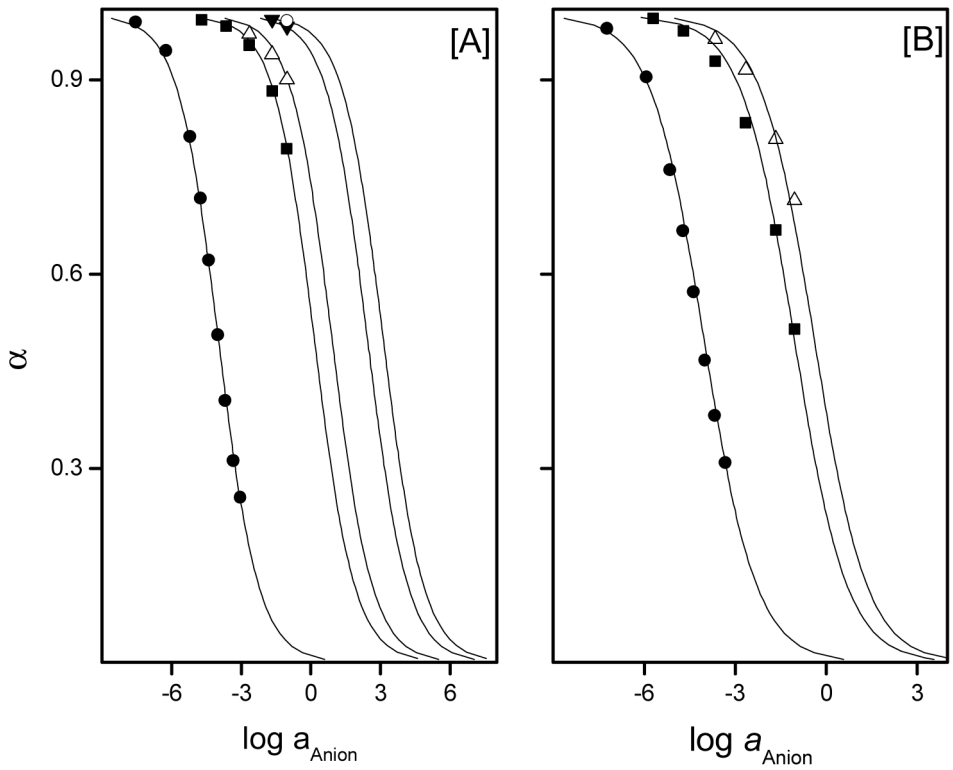

Fig. 6.

Optical response of Film-6, [A], and Film-7, [B], towards various anions as measured in 100 mM β-alanine-phosphate buffer, 1 mM CDTA, pH 3.6: (●) fluoride, (■) thiocyanate, (△) perchlorate, (▼) nitrate ~ nitrite, and (○) bromide ~ chloride ~ sulfates. Solid lines are the theoretical response curves of the fluoride optical sensing film toward various anions calculated using eq. 2. Absorbance values at 537 nm were employed to calculate α values

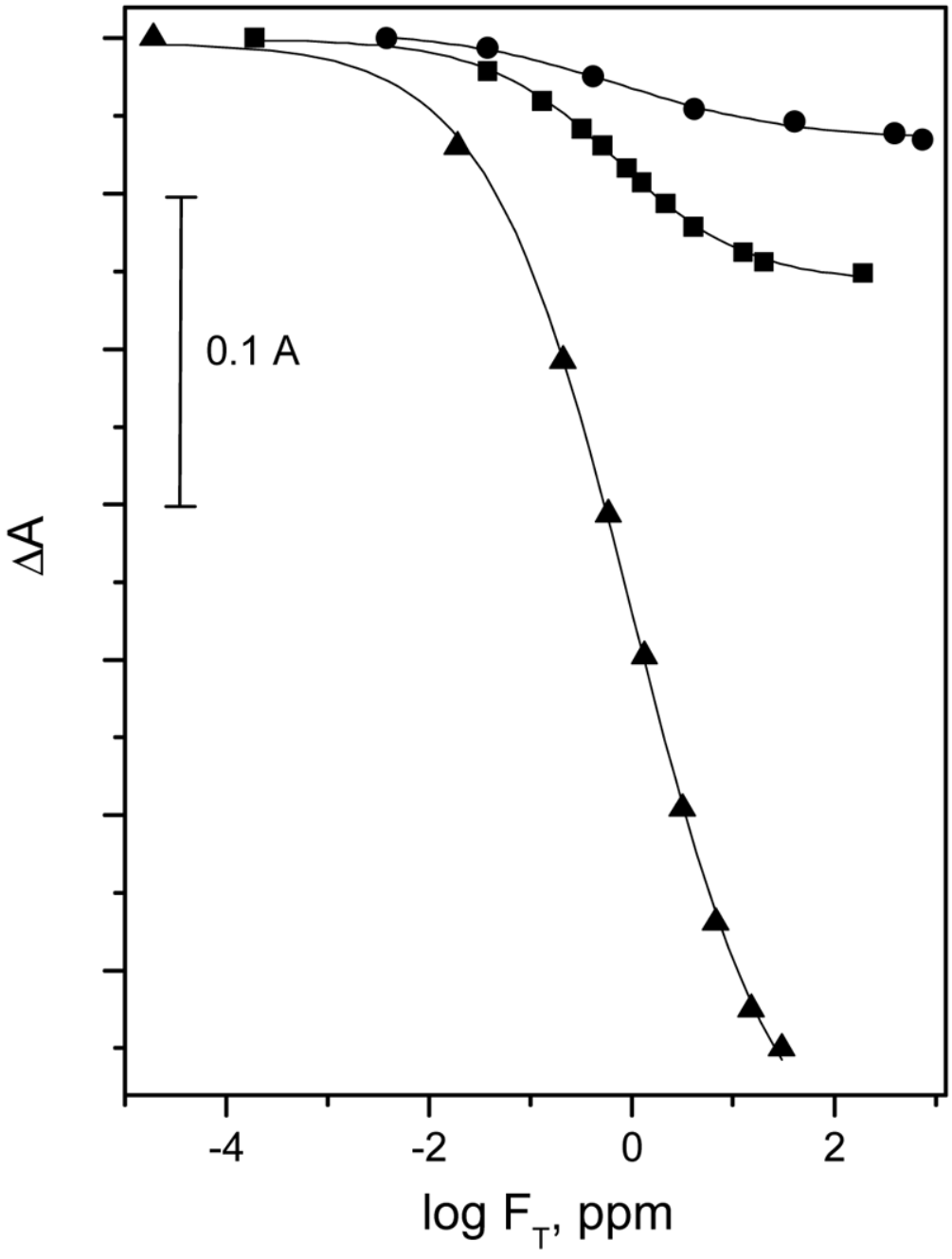

Fig. 7.

Absorbance changes of Al[OEP]/ETH-7075 based fluoride optical sensitive films, at λ_{max} of the deprotonated from of the pH chromoionophore, as a function of fluoride ion concentration using different film compositions: Film-4 (●), Film-5 (■), and Film-6 (▲)

Table 1

Composition of Bulk-Optode Films Used in This Study.[a]

	Plasticizer	Al[OEP], μmol/g	ETH-7075, μmol/g	KTFPB, μmol/g
Film-1	*o*-NPOE	16	-	-
Film-2	*o*-NPOE	16	-	8
Film-3	*o*-NPOE	16	-	16
Film-4	*o*-NPOE	16	16	-
Film-5	*o*-NPOE	24	24	-
Film-6	*o*-NPOE	72	72	-
Film-7	DOS	72	72	-

[a] All optical films were prepared using a 1:2 PVC to plasticizer mass ratio.

Table 2

Selectivity Coefficients of Al[OEP]/ETH-7075 Based Fluoride Optical Sensing Films, Measured in 100 mM β-Alanine-Phosphate Buffer, 1 mM CDTA, pH 3.60, in Comparison with the Potentiometric Selectivity Coefficients of Zr(IV)[OEP], and Ga(III)[OEP] Membrane Electrodes.

Anion	$\log K_{\text{Fluoride, Anion}}$ (Required)	$\log K^{\text{opt}}_{\text{Fluoride,Anion}}$		$\log K^{\text{pot}}_{\text{Fluoride,Anion}}$	
		Al[OEP], Film-6	Al[OEP], Film-7	Zr(IV)[OEP] ISE[a]	Ga(III)[OEP] ISE[b]
F^-	0.0	0.0	0.0	0.0	0.0
SO_4^{2-}	−4.7	≤−7.1	-	-	-
Cl^-	−4.8	≤−7.1	-	−5.1 (−4.3)	−2.9
NO_3^-	−3.2	−6.4	-	−2.4 (−1.8)	−2.3
NO_2^-	−2.3	−6.4	-	-	−0.77
Br^-	-	≤−7.1	-	−3.4 (−2.7)	-
SCN^-	-	−4.2	−3.0	−0.5 (0.3)	0.53
ClO_4^-	-	−4.5	−3.6	0.4 (0.9)	2.0

[a] Data from (ref.22) for Zr(IV)[OEP] as a charged carrier, and data in parenthesis are from (ref.23) for Zr(IV)[OEP] as a neutral carrier

[b] From (ref.20)

Table 3

Determination of Fluoride in Drinking Water Samples Using Al[OEP]/ETH-7075 Based Fluoride Optical Sensitive Membrane, Film-6, and LaF_3 ISE in 100 mM β-Alanine buffer, pH 3.60, 1 mM CDTA.

Sample	Al[OEP]/ETH-7075		LaF_3-ISE	
	ppm	c.v., %[a]	ppm	c.v., %[a]
1	0.73	2.5	0.70	0.42
2	0.51	2.1	0.54	0.42
3	0.46	3.2	0.47	0.64
4	0.36	2.9	0.39	0.75
5	0.12	3.1	0.16	0.75

[a](c.v. is the coefficient of variance, n = 3)